

## Exclusive processes at JLab at 6 GeV

Andrey Kim<sup>1,a</sup>

<sup>1</sup>University of Connecticut

**Abstract.** Deeply virtual exclusive reactions provide a unique opportunity to probe the complex internal structure of the nucleon. They allow to access information about the correlations between parton transverse spatial and longitudinal momentum distributions from experimental observables. Dedicated experiments to study Deeply Virtual Compton Scattering (DVCS) and Deeply Virtual Meson Production (DVMP) have been carried out at Jefferson Lab using continuous electron beam with energies up to 6 GeV. Unpolarized cross sections, beam, target and double spin asymmetries have been measured for DVCS as well as for  $\pi^0$  exclusive electroproduction. The data from Hall B provide a wide kinematic coverage with  $Q^2=1-4.5$  GeV<sup>2</sup>,  $x_B=0.1-0.5$ , and  $-t$  up to 2 GeV<sup>2</sup>. Hall A data have limited kinematic range partially overlapping with Hall B kinematics but provide a high accuracy measurements. Scaling tests of the DVCS cross sections provide solid evidence of twist-2 dominance, which makes chiral-even GPDs accessible even at modest  $Q^2$ . We will discuss the interpretation of these data in terms of Generalized Parton Distributions (GPDs) model. Successful description of the recent CLAS  $\pi^0$  exclusive production data within the framework of the GPD-based model provides a unique opportunity to access the chiral-odd GPDs.

### 1 Introduction

In recent years, parton distribution functions have been generalized to contain information not only on the longitudinal but also on the transverse distributions of partons in a fast moving hadron. The Generalized Parton Distributions (GPDs) [1–3] add important piece of information that is missing in one-dimensional parton densities, in particular, distribution of partons in the plane transverse to the direction of motion. They are also closely related to the nucleon electromagnetic form factors and contain information that cannot be accessed by either of these quantities. The most important aspect is that GPDs can provide detailed knowledge about the space-momentum distributions of quarks and gluons within the nucleon and about the contribution of quark orbital angular momentum to the nucleon spin. GPDs contain the information needed to construct a multi-dimensional image of the internal structure of the nucleon.

Deeply virtual exclusive processes where the photon virtuality  $Q^2$  is large, have emerged as a powerful probe to study the nucleon structure at the parton level. In Bjorken scaling regime, the scattering amplitude of hard exclusive processes, such as Deeply Virtual Compton Scattering (DVCS) and Deeply Virtual Meson Production (DVMP), factorizes into a hard scattering part and soft part described by Generalized Parton Distributions. This opens the prospect of using exclusive meson electroproduction processes as a means to systematically explore the quark structure of the nucleon. Schematic illustrations for DVCS and DVMP in handbag framework are shown on Fig. 1.

While DVCS has most extensively been studied theoretically [1, 4, 5] and experimentally [6–9] to constrain the leading order GPDs, DVMP offers the advantage of filtering certain GPDs and also has evolved into an important process giving access to higher-twist mechanisms.

In general, there are four chiral-even GPDs ( $H$ ,  $\tilde{H}$ ,  $E$ ,  $\tilde{E}$ ) involved in the parton helicity-conserving processes and four chiral-odd GPDs that correspond to parton helicity-flip processes ( $H_T$ ,  $\tilde{H}_T$ ,  $E_T$ ,  $\tilde{E}_T$ ). At leading twist of the GPD framework, DVCS amplitudes couple only to transverse photons and sensitive to chiral-even GPDs  $H$ ,  $\tilde{H}$  and  $E$ , while the neutral pseudoscalar DVMP amplitudes couple only to longitudinally polarized photons and these channels are sensitive only to the chiral even GPDs  $\tilde{H}$ ,  $\tilde{E}$  in the nucleon [10, 11]. The last two GPDs contain information about the spatial distribution of the quark spin. The early theoretical efforts to explain the pseudoscalar DVMP focused on these  $\tilde{H}$  and  $\tilde{E}$  GPDs at leading twist. However, Hall-B at Jefferson Lab measured surprisingly large  $\pi^0$  beam spin asymmetry (BSA) values that strongly suggests substantial contributions from transversely polarized photons [12], otherwise BSA should be zero or very small. These contributions can be calculated within a handbag approach as the convolutions of leading-twist chiral-odd GPDs with a twist-3 meson distribution amplitude [13–15]. The recent publication of CLAS collaboration on measurements of exclusive  $\pi^0$  electroproduction structure functions [16] showed strong sensitivity to transversity GPDs.

The GPDs themselves are not accessible directly from the experiment. In fact, the measured cross sections de-

<sup>a</sup>e-mail: kenjo@jlab.org

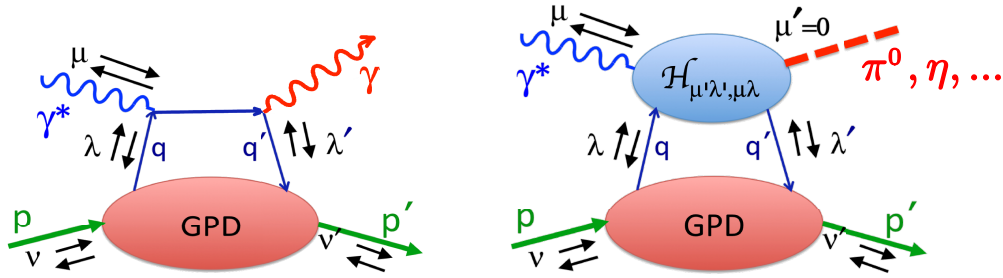


**Figure 1.** Schematic DVCS (left) and DVMP (right) in the handbag mechanism framework. The helicities of initial (final) nucleon and quark are denoted as  $\nu$  ( $\nu'$ ) and  $\lambda$  ( $\lambda'$ ) respectively. The incident virtual photon and produced photon (meson) have  $\mu$  and  $\mu'$  helicities.

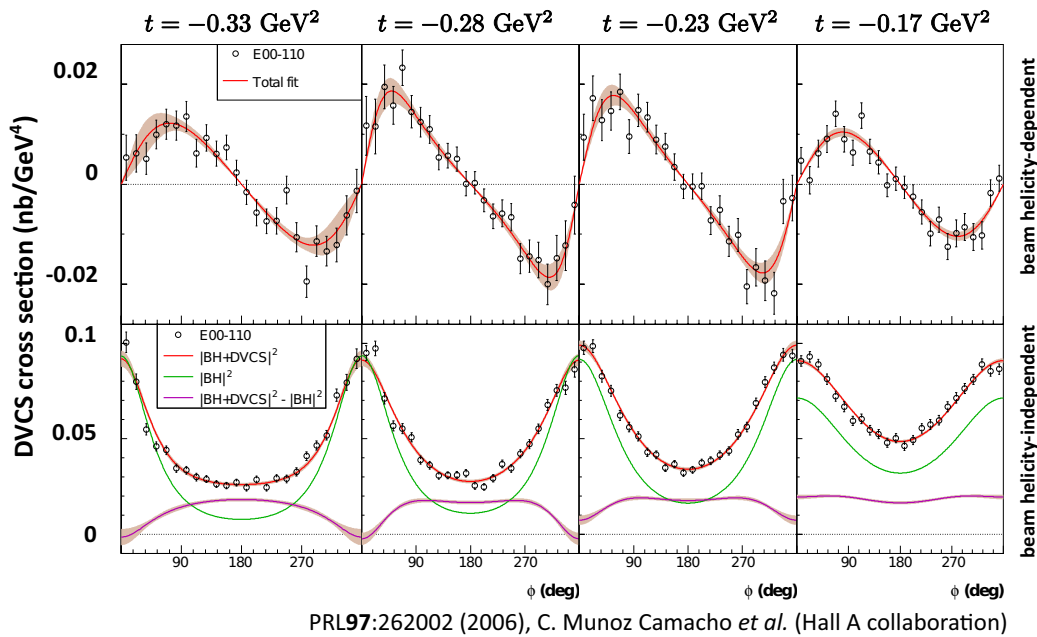


**Figure 2.** Helicity dependent (top) and independent (bottom) DVCS cross sections from Hall A, JLab at  $Q^2 = 3.4 \text{ GeV}^2$  and four different  $t$  bins as a function of  $\phi$ . Error bars show statistical uncertainties. The curves are explained in the graph. Please note the clear signature of DVCS contribution above the Bethe-Heitler background.

pend on the convolutions of hard part and soft GPDs part (called Compton Form Factors for DVCS), and they are the quantities that are extractable from DVCS and DVMP experiments. These convolutions are the functions of  $\xi$  and momentum transfer  $t$ . The variable  $x$  is integrated over and can not be accessed experimentally.

## 2 Deeply Virtual Compton Scattering

The JLab Hall A collaboration presented first measurements of the  $\bar{e}p \rightarrow ep\gamma$  cross sections in the valence quark region [17] (see on Fig. 2). The experiment E00-110 ran in Hall A [18] at JLab with 5.75 GeV longitudinally polarized electron beam and 15 cm liquid  $H_2$  target. As it is impossible to separate Bethe-Heitler (BH) and DVCS processes experimentally one measures both processes, as well as their interference, and then removes the contribution from pure BH term as it is exactly calculable in

terms of the nucleon form factors [3, 19]. The cross sections for DVCS on proton were measured for three kinematic points at  $Q^2=1.5, 1.9$  and  $2.3 \text{ GeV}^2$ . The DVCS helicity-independent and helicity-dependent cross sections provide access to the real and imaginary part of BH-DVCS interference term respectively. Azimuthal dependence of helicity-dependent cross section allows the separation of twist-2 and twist-3 contributions in the DVCS-BH interference terms. Fig. 3(left) shows the  $Q^2$  dependence of the imaginary angular harmonics over the full  $t$  domain. The right plot displays the twist-2 angular harmonics as a functions of  $t$ , together with the predictions from a model of Vanderhaeghen, Guichon and Guidal (VGG) [19–21]. The absence of  $Q^2$  dependence provides crucial support for the dominance of the twist-2 in DVCS amplitude at modest  $Q^2$ .

The JLab CLAS collaboration measured beam spin asymmetry (BSA) [22] (see Fig. 4) in the reaction  $\bar{e}p \rightarrow$

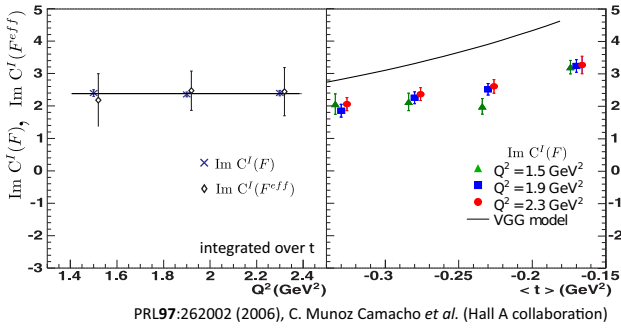


**Figure 3.** Left:  $Q^2$  dependence of imaginary parts of (twist-2)  $C^I(F)$  and (twist-3)  $C^I(F^{eff})$  angular harmonics, averaged over  $t$ . The horizontal line is the fitted average of  $\text{Im}[C^I(F)]$ . Right: Extracted real and imaginary parts of the twist-2 angular harmonics as a function of  $t$ . The theoretical predictions are from the Ref. [19–21].

$e\gamma$  using longitudinally polarized electron beam with 5.77 GeV energy, 2.5 cm-long liquid-hydrogen target and CLAS spectrometer [23]. Neglecting a twist-3 DVCS term, this asymmetry arises from the interference from BH and DVCS processes that is sensitive to the specific combination of the proton GPDs  $H$ ,  $\tilde{H}$  and  $E$ . The GPD  $H$  provides the dominant contribution to the beam spin asymmetry, thus, neglecting the small contribution from other GPDs, BSA can be expressed as a function of only  $H$ .

The first measurements of longitudinal target spin asymmetries (TSA) were published by CLAS collaboration [24] (see Fig. 5) using 5.7 GeV electron beam and longitudinally polarized NH<sub>3</sub> target. A significant azimuthal dependence of BH-DVCS interference term yields directly to the dominant combination of GPDs  $H$  and  $\tilde{H}$ , with other GPDs being kinematically suppressed.

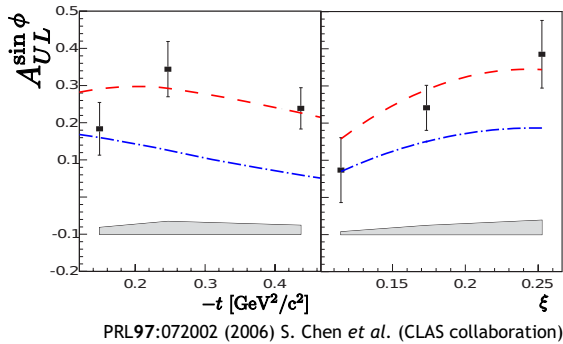


**Figure 5.** The  $-t$  (left) and  $\xi$  (right) dependence of the  $\sin\phi$  moment of target spin asymmetry for DVCS. The dashed curves represent VGG model predictions using  $\xi$ -dependent GPD parametrization. The dotted curves show the asymmetries when  $\tilde{H}=0$ .

The wide kinematic coverage of CLAS is particularly important as it allows the global analysis of measured observables and a model-independent extraction of DVCS amplitudes. For example, BSA is especially sensitive to the GPD  $H$ . Combined with TSA that is sensitive to  $H$  and  $\tilde{H}$ , it allows to constrain the contribution from  $\tilde{H}$  alone.

### 3 Deeply Virtual $\pi^0$ Production

Although DVCS is the cleanest process to access GPDs, the variety of DVMP channels allows to perform quark flavor separation of GPDs. In addition, pseudoscalar meson electroproduction, particularly  $\pi^0$  production in the reaction  $ep \rightarrow e'p'\pi^0$ , was identified as especially sensitive to the parton helicity-flip subprocesses. While the interpretation of  $\pi^+$  production is complicated by the dominance of the longitudinal  $\pi^+$ -pole term, the  $\pi^0$  production, where that contribution is absent, may become a unique source of information on transversity GPDs [14, 25].

Beam spin asymmetries for exclusive  $\pi^0$  electroproduction were measured by CLAS collaboration in the wide kinematic range [26] (see Fig. 7). The measured asymmetries are of the order of 0.04 to 0.11, and, in particular, show no decrease as a function on  $Q^2$ . This is a clear sign of significant contribution from  $LT'$  interference, that can not be calculated within the formalism where only longitudinal amplitude, dominant in the Bjorken regime, is considered. These nonzero asymmetries imply that both transverse and longitudinal amplitudes participate in the process.

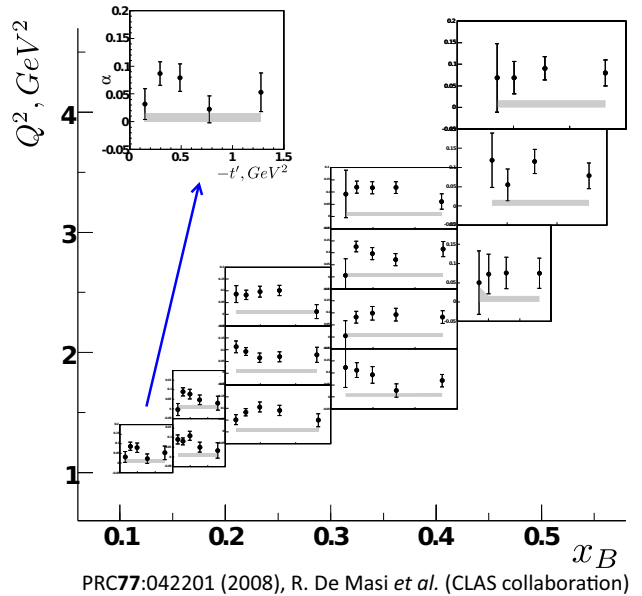


**Figure 7.** Schematic DVCS (left) and DVMP (right) in the hand-bag mechanism framework. The helicities of initial (final) nucleon and quark are denoted as  $\nu$  ( $\nu'$ ) and  $\lambda$  ( $\lambda'$ ) respectively. The incident virtual photon and produced photon (meson) have  $\mu$  and  $\mu'$  helicities.

During the past few years, two parallel approaches have been developed utilizing chiral odd GPDs in the calculation of pseudoscalar electroproduction: the Goloskokov-Kroll (GK) model [14, 25, 27] and Goldstein-Liuti (GL) model [28]. Although different in details they both lead to sizable transverse photon amplitudes, as evidenced in the CLAS data. Inclusion of the chirally-odd twist-3 components of the hard exclusive amplitude gives results in fair agreement with the measured cross sections [29] (see Fig. 6). A combination of  $\tilde{H}_T$  and  $E_T$  plays a

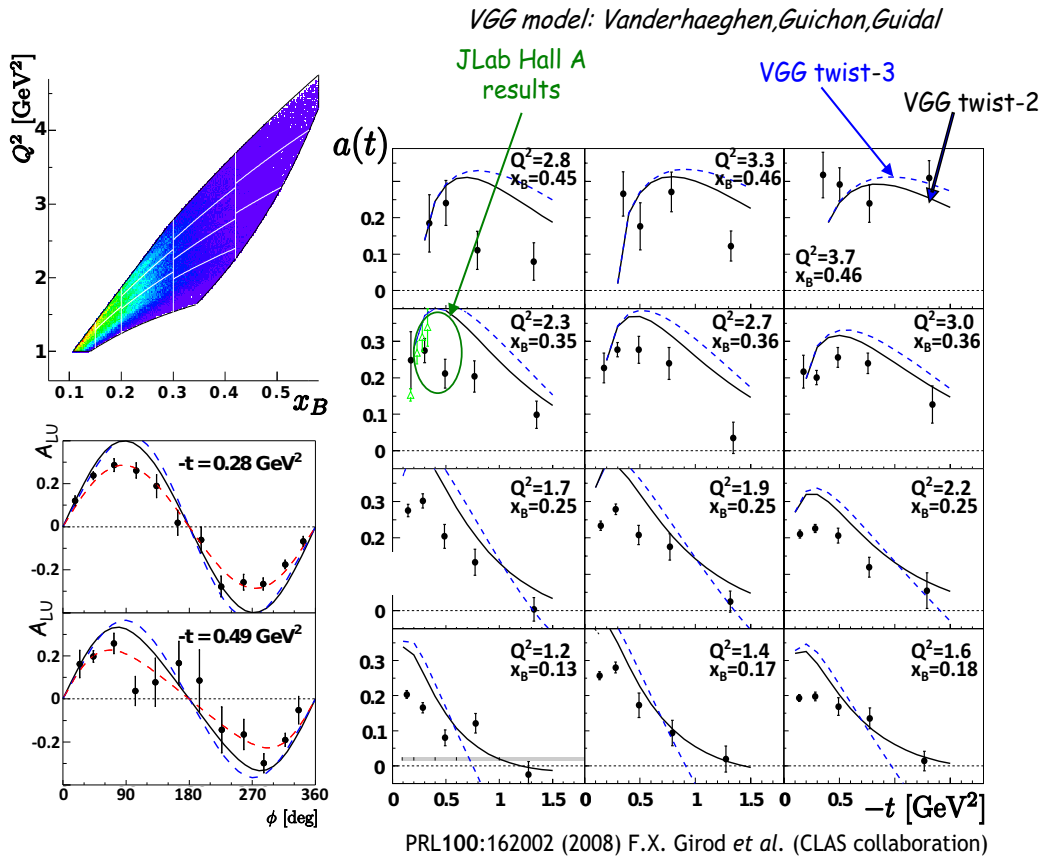


**Figure 4.** Left top panel shows the kinematic coverage and binning in  $Q^2, x_B$  space. Left bottom panel shows the beam spin asymmetries as a function of  $\phi$  for two of the 62 ( $Q^2, x_B, t$ ) bins corresponding to the  $\langle x_B \rangle = 0.25, \langle Q^2 \rangle = 1.95$  GeV<sup>2</sup> and two values of  $\langle t \rangle$ . Right: beam spin asymmetries at  $90^\circ$  as a function of  $-t$ . Each individual plot corresponds to a bin in  $Q^2, x_B$ . The red-dashed curves correspond to the fit. The black (blue) curves correspond to the GPD calculation at twist-2 (twist-3) levels, with  $H$  contribution only.

particularly prominent role. The cross section behaviour in low  $-t$  region is determined by interplay between these two GPDs. The comparison between data and model predictions shows the sensitivity of measured  $\pi^0$  structure functions for constraining the chiral-odd GPDs.

The analysis of experimental data on exclusive  $\pi^0$  electroproduction is underway to extract longitudinal target spin asymmetries as well as double spin asymmetries. The experiment ran in 2009 in Hall B, JLab using longitudinally polarized electron beam and longitudinally polarized solid NH<sub>3</sub> target. The unpolarized and polarized structure functions can be expressed as a combinations of the partonic subprocess amplitudes and GPDs convolutions. Therefore measurements of beam, target and double spin asymmetries and extraction of azimuthal moments provide several observables, combined analysis of which may allow separation of contributions from different underlying GPDs.

## 4 Conclusion

The dedicated experiments to measure DVCS and DVMP at Jefferson Lab with 6 GeV electron beam provide a large set of experimental data over a wide kinematic range. Combined together they allow access to chiral even as well

as chiral odd GPDs. The initial interpretations of deep exclusive processes in terms of Generalized Parton Distributions models are already showing remarkable results.

The successful description of unpolarized cross sections for pseudoscalar meson production by CLAS provides a unique opportunity to access chiral odd GPDs. The precise calculations of polarized spin observables, however, are not feasible at present. Theoretical calculations of  $\pi^0$  electroproduction based on the GPDs inspired models include many uncertainties such as parametrization of the chiral odd GPDs, treatment of the higher twist contributions and the reaction mechanisms (*e.g.*, corrections to the partonic mechanism from hadronic-size configurations in high- $Q^2$  production). The extractions of structure functions for various DVMP channels would increase number of experimental observables used for model-independent constraints and further clarify the discrepancies between data and model calculations.

The work presented here leads directly to the program of the Jefferson Lab 12 GeV upgrade. The increased energy and luminosity will allow higher accuracy measurements over significantly wider kinematic range providing us with the opportunity to extend our analysis at higher  $Q^2$  and test the mechanism of exclusive photon and meson electroproduction.

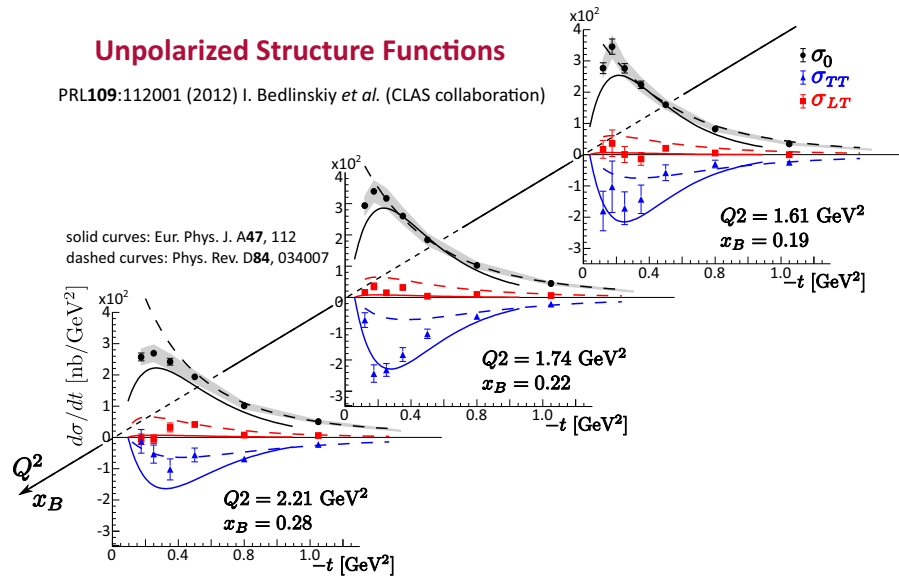


**Figure 6.** The extracted structure functions for exclusive  $\pi^0$  electroproduction as a functions of  $t$  for the bins with best kinematic coverage. The curves are theoretical predictions and explained on the graph. The shaded bands represent experimental systematic uncertainties.

## References

- [1] X.D. Ji, Phys. Rev. Lett. **78**, 610 (1997), hep-ph/9603249
- [2] A.V. Radyushkin, Phys. Lett. **B380**, 417 (1996), hep-ph/9604317
- [3] A.V. Belitsky, D. Mueller, A. Kirchner, Nucl. Phys. **B629**, 323 (2002), hep-ph/0112108
- [4] A. Radyushkin, Phys. Rev. D **56**, 5524 (1997)
- [5] D. Mueller et al., Fortsch. Phys. **42**, 101 (1994)
- [6] S. Stepanyan et al. (CLAS), Phys. Rev. Lett. **87**, 182001 (2001)
- [7] C. Camacho et al., Phys. Rev. Lett. **97**, 262002 (2006)
- [8] F. Girod et al., Phys. Rev. Lett. **100**, 162002 (2008)
- [9] G. Gavalian et al., Phys. Rev. C **80**, 035206 (2009)
- [10] M.I. Eides, L.L. Frankfurt, M.I. Strikman, Phys.Rev. **D59**, 114025 (1999)
- [11] L. Mankiewicz et al., Eur. Phys. J. C **10**, 307 (1999)
- [12] R. De Masi et al. (CLAS), Phys. Rev. C **77**, 042201 (2008)
- [13] S. Ahmad, G.R. Goldstein, S. Liuti, Phys. Rev. **D79**, 054014 (2009), 0805.3568
- [14] S. Goloskokov, P. Kroll, Eur.Phys.J. **A47**, 112 (2011), 1106.4897
- [15] G.R. Goldstein, J.O.G. Hernandez, S. Liuti, Phys. Rev. D **84**, 034007 (2011)
- [16] I. Bedlinskiy et al. (CLAS), Phys. Rev. Lett. **109**, 112001 (2012)
- [17] C. Munoz Camacho et al. (Jefferson Lab Hall A), Phys. Rev. Lett. **97**, 262002 (2006), nucl-ex/0607029
- [18] J. Alcorn, B. Anderson, K. Aniol, J. Annand, L. Auerbach et al., Nucl.Instrum.Meth. **A522**, 294 (2004)
- [19] K. Goeke, M.V. Polyakov, M. Vanderhaeghen, Prog. Part. Nucl. Phys. **47**, 401 (2001), hep-ph/0106012
- [20] M. Vanderhaeghen, P.A.M. Guichon, M. Guidal, Phys. Rev. **D60**, 094017 (1999), hep-ph/9905372
- [21] M. Guidal, M.V. Polyakov, A.V. Radyushkin, M. Vanderhaeghen, Phys. Rev. **D72**, 054013 (2005), hep-ph/0410251
- [22] F.X. Girod et al. (CLAS), Phys. Rev. Lett. **100**, 162002 (2008), hep-ex/0711.4805
- [23] B. Mecking et al. (CLAS Collaboration), Nucl.Instrum.Meth. **A503**, 513 (2003)
- [24] S. Chen, H. Avakian, V. Burkert et al. (CLAS), Phys. Rev. Lett. **97**, 072002 (2006), hep-ex/0605012
- [25] S.V. Goloskokov, P. Kroll, Eur. Phys. J. **C65**, 137 (2010), 0906.0460
- [26] R. De Masi et al. (CLAS Collaboration), Phys.Rev. **C77**, 042201 (2008), 0711.4736
- [27] S.V. Goloskokov, P. Kroll, Eur. Phys. J. **C53**, 367 (2008), hep-ph/0708.3569
- [28] G. Goldstein, J.O.G. Hernandez, S. Liuti, to be published (2013), 1311.0483
- [29] I. Bedlinskiy et al. (CLAS Collaboration), Phys.Rev.Lett. **109**, 112001 (2012), 1206.6355